Eur. J. Mech., A/Solids, **16**, special issue, 65-82, 1997

Compressive failure of composites due to microbuckle growth

N. A. FLECK *, S. SIVASHANKER * and M. P. F. SUTCLIFFE *

ABSTRACT. - The compressive failure of unidirectional and multi-directional carbon fibre reinforced composites is investigated experimentally and theoretically. Failure is by microbuckle growth, and can be modelled adequately by a large scale crack bridging model comprising a crack tip toughness and constant crack bridging stress. The effect of fibre and matrix properties on microbuckle propagation is explored for unidirectional material: brittle fibres break whereas fibres of higher failure strain bend without fracture during microbuckling. The mechanism of microbuckle propagation in multi-directional material is explored: the microbuckles within the 0^o plies are accompanied by delamination with neighbouring plies, and are reminiscent of wing-crack formation in brittle heterogeneous solids. The investigation provides strong evidence that microbuckles propagate in a crack-like fashion with band broadening along the flanks of the microbuckle, for both unidirectional and multi-directional composites.

1. Introduction

Polymer matrix - fibre reinforced composites are increasingly used in a wide range of applications (for example aerospace, sports goods, pleasure boats, small ships and submarines) where high strength and high stiffness are required at low weight. The high as-manufactured cost of the material precludes more widespread use in general engineering. A lack of knowledge of material behaviour is compensated for by additional safety factors and large test programmes.

A major design-limiting feature of polymer matrix composites is their relatively low compressive strength in relation to their tensile strength. Thus a composite beam in bending, such as an aircraft wing structure, is likely to fail in compression rather than in tension. Over the past decade intensive research has been conducted into the compressive failure of composites and the accepted dominant failure mechanisms are accepted to be *buckle-delamination* in a composite with a large initial delamination in a near-surface ply, and *microbuckling* for a composite with no large initial delaminations. Microbuckling is associated with non-linear shear of the polymer matrix and initiates from regions of pre-existing fibre waviness (of magnitude only a few degrees). Ceramic and metal matrices have much higher stiffnesses and strengths than polymer matrices, and compressive failure is by

* Cambridge University Engineering Dept., Trumpington St., Cambridge CB2 1PZ, England.

0997-7538/97/$ 7.00/

other mechanisms: for example, crushing within the individual fibres for metal matrix composites and tensile cracking of the matrix for ceramic matrix composites.

An open question has been whether a microbuckle propagates as a *crack-like* feature or as a *dislocation-like* feature in large sheet structures under prescribed load. Early models (for example, Fleck and Budiansky (1991)) emphasised the fact that material within a microbuckle band locks-up through a resistance to volumetric compression within the band. If the microbuckle is of fixed width, then the locked-in shear displacement across the microbuckle is constant along the flanks of the growing microbuckle, and the microbuckle will propagate in a dislocation-like manner under a constant remote stress (analogous to the Peierls stress for the motion of a dislocation on a slip plane). Alternatively, if the microbuckle propagates with an increasing width along its wake, then the shear displacement across the microbuckle increases with distance behind the microbuckle tip, and the microbuckle is akin to a crack. The notion of band broadening of a microbuckle under constant applied stress has been emphasised by Moran *et al.* (1995) in experiments on IM7/PEEK composites. Their IM7 fibres were sufficiently strong not to fail during the microbuckling process, and they observed that a microbuckle broadens under constant remote stress. Recent experimental observations (Sutcliffe and Fleck, 1994; Sivashanker *et al.*, 1996) show that a microbuckle in unidirectional T800/924C carbon-epoxy propagates in a crack-like mode with a constant bridging stress across it and a constant crack tip toughness. The generality of this model is examined in the present work: we investigate experimentally the mode of microbuckle growth for a range of unidirectional carbon fibre composites, and for a range of laminate lay-ups. The single-edge notch specimen configuration used in this investigation simulates in an approximate manner sharp stress raisers in aircraft panels such as cut-outs. Section 2 describes the experimental procedures used. Sections 3 and 4 present experimental results for the uni- and multi-directional material, respectively.

2. Experimental measurement of microbuckle propagation

Microbuckle propagation is examined for three types of unidirectional carbon fibre reinforced composite: (i) Toray T800 carbon fibres in a Ciba Geigy 924C toughened epoxy, (ii) AS4 carbon fibres in a thermoplastic PEEK matrix APC2, and (iii) IM8 fibres in APC2 PEEK matrix. This allows the effects of fibre and matrix properties to be explored separately. The IM8 fibres have a significantly larger failure strain than the AS4 and T800 fibres. The PEEK matrix has a greater ductility than the 924C toughened epoxy. The effect of lay-up was examined by testing three types of laminate made from T800/924C composite: $[(\pm 45/0_4)_2]_s$ which contains 67% of 0° plies, $[(\pm 45/0_2)_3]_s$ which contains 50% of 0° plies and $[(\pm 45/0/90)_3]_s$ which contains 25% of 0° plies.

2.1 Experimental Method

An edge-notch, 15 mm long and 3 mm wide, was machined in specimens of 50 mm width and 3 mm thickness, see Fig. 1. Aluminium end tabs were bonded to these specimens using a hot-cure epoxy adhesive to enable a smooth transfer of load from wedge grips into the specimens. In conventional notched-compression tests of composites, microbuckle initiation occurs in a catastrophic fashion and it is very difficult to observe microbuckle growth from the notch root. This problem was overcome by initiating a 2 mm long microbuckle by local indentation at the notch root, prior to uniaxial loading of the specimen. An indent was made at the root of the starter notch using a 2 mm roller in a three point bend fixture. The outer supporting rollers were of much larger diameter to distribute the contact load, thus preventing premature crushing of the specimen at these rollers.

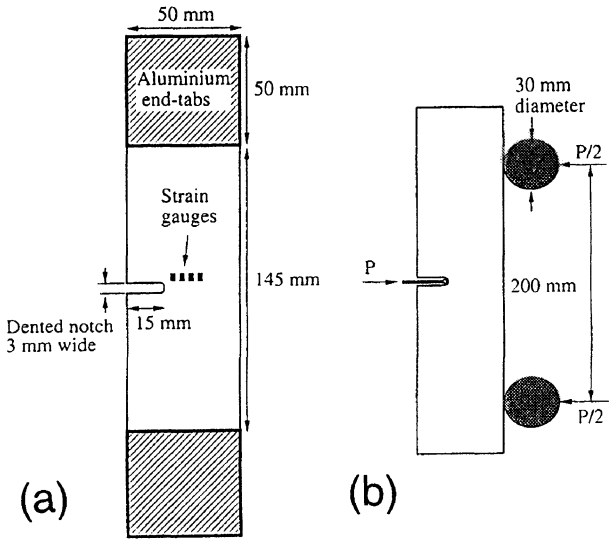

Fig. 1. - (a) Specimen geometry. (b) The three point bend loading arrangement used to nucleate a microbuckle.

The specimen was loaded in compression using a screw-driven test machine in displacement control. Anti-buckling guides, lubricated with PTFE spray, were used to prevent Euler macrobuckling of the specimen without inducing too much friction. Foil strain gauges were placed on the rear-face 2 mm above the expected microbuckle trajectory to measure the local bridging stresses across the growing microbuckle. A high magnification video recorder was used to record the sequence of damage events, including the length of the microbuckle zone as a function of applied load. The initial loading rate was 0.01 mm/s and, upon the first sign of microbuckle propagation the loading rate was reduced to 0.001 mm/s to slow down the stable

propagation. When the microbuckle had propagated part-way through the ligament, the specimens were unloaded and the test was terminated.

3. Experimental Observations for Unidirectional Material

3.1 Failure modes

For all unidirectional specimens, the microbuckle zone is confined to a narrow wedge-shaped localised band emanating from the single edge notch. A macroscopic view of the growing microbuckle is shown in Fig. 2 for AS4/PEEK. The T800 fibres in the T800/924C material and the AS4 fibres of the AS4/PEEK material have sufficiently low ductility for them to fail in bending during microbuckling: fibre fracture occurs on successive planes leading to multiple kink-band formation as the microbuckle band widens. This has been noted previously for T800/924C composite (Sutcliffe and Fleck, 1994) and is discussed by Sivashanker *et al.* (1996). In contrast, the IM8 fibres of the IM8/PEEK composite remain intact during microbuckling and the microbuckle band broadens without fibre fracture, in the manner described by Moran *et al.* (1995).

At the macroscopic level, there is no significant difference in appearance of microbuckle growth in the three unidirectional composites, and the wedge-shaped microbuckle propagates in an out-of-plane manner, as sketched in Fig. 3. Portions of the specimen above and below the microbuckle slide past each other in the through-thickness direction. Out-of-plane microbuckling is expected since there is less constraint in the through-thickness direction (which is 3 mm thick) compared to the ligament width of 35 mm.

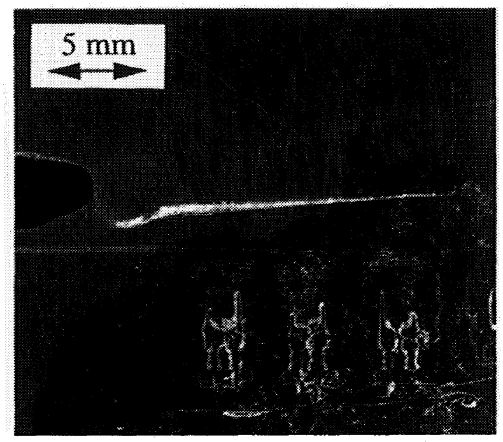

Fig. 2. - Side view of unidirectional AS4/PEEK specimen, at end of test. Note the strain gauge positions.

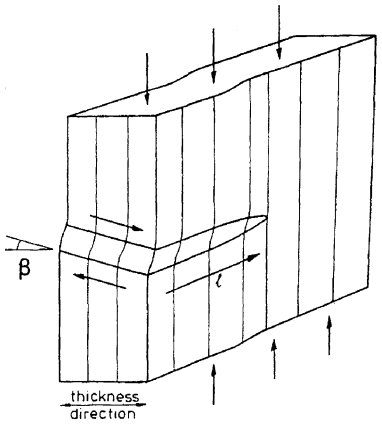

Fig. 3. - Sketch of out-of-plane microbuckling in unidirectional composites, with material above and below the kink-band sliding against each other under uniaxial compression.

The extent of this sliding decreases towards the microbuckle tip suggesting that the microbuckle is similar to a mode I crack in compression. The orientation of the kink band was measured to be in the range $\beta = 25^o$ - 27^o for the three unidirectional materials.

The evolution of microbuckle length with remote applied stress is shown in Fig. 4 for the three unidirectional composites of the current study. There is only a small effect of material composition upon the collapse response, with the IM8/PEEK behaving in a stronger manner than the AS4/PEEK. In broad terms, microbuckle growth occurs at an approximately constant applied stress of 150-200 MPa, which is almost an order of magnitude less than the stress required to initiate microbuckling in unidirectional material (for example, the compressive strength of unnotched T800/924C unidirectional composite is about 1600 MPa).

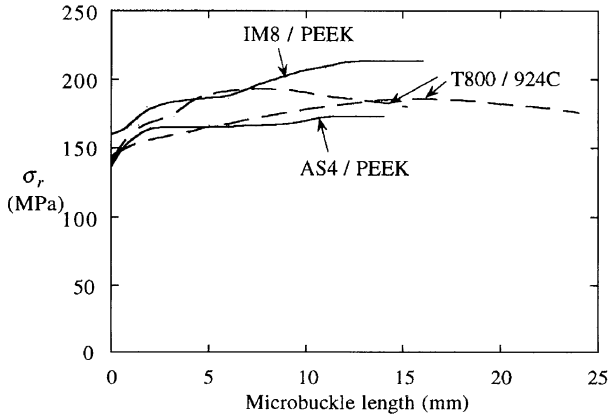

Fig. 4. - R-curve behaviour for the three unidirectional laminates.

At the end of each test, the width of the microbuckle band in the axial direction was measured using a scanning electron microscope to derive the variation in the band width as a function of distance from the microbuckle tip. Similar results were found for all three materials in the study. Sivashanker *et al* (1996) have presented the results previously for the T800/924C composite. Figures 5a and 5b show the corresponding curves for AS4/PEEK and IM8/PEEK. Remarkably, the width of the microbuckle band increases to almost 1 mm at a distance of 10-15 mm behind the microbuckle tip. For the T800/924C and AS4/PEEK the number of discrete kink band fragments within the overall microbuckle band increases with distance along the microbuckle flanks from unity at the microbuckle tip to about 6 in the vicinity of the notch root. The width of the individual kink band fragments is constant at about 150 μm, or about 25 fibre diameters, in agreement with the predictions of Fleck *et al.* (1995a). The continued increase in microbuckle width with distance back from the tip strongly suggests that the microbuckle can be modelled as a bridged crack; this is detailed below.

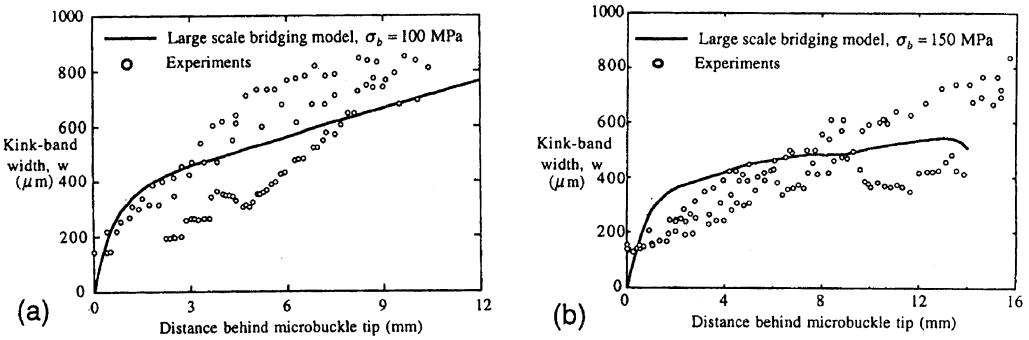

Fig. 5. - Microbuckle shape for (a) 10 mm long microbuckle in AS4/PEEK, and (b) 16 mm long microbuckle in IM8/PEEK.

3.2 Measured bridging stresses

The bridging stresses across the flanks of the growing microbuckle are deduced from strain gauge measurements, and are shown in Fig. 6 as a function of distance from the microbuckle tip to the strain gauge. There is a negligible effect of material composition on response. In each case, the stress across the microbuckle has a maximum in the vicinity of the microbuckle tip, and levels off at 100-150 MPa when the propagating microbuckle tip is sufficiently distant from the gauges. This response suggests that the microbuckle can be treated as a crack with a constant crack bridging stress across its flanks.

3.3 Discussion of unidirectional results

We note that there is no marked variation in the microbuckle propagation stress with material composition, despite differences in fibre fracture behaviour. In contrast, the compressive strength of unnotched AS4/APC2 is 30% less that of T800/924C, and the compressive strength of IM8/PEEK is 20% that of T800/924C.

The steady state band broadening stress is about 2-3 times the shear yield strength for the 924C matrix and PEEK matrix, in agreement with the predictions of a work calculation (Fleck, 1997). Confirmation that the IM8/PEEK material did not suffer fibre fracture came from tensile tests on small specimens containing a microbuckle band across the full section, cut from a parent compression specimen. The residual tensile strength was about 150 MPa. This low value is thought to be associated with bending failure of the fibres at the boundaries of the microbuckle band.

3.4 Crack-bridging model of microbuckling

In this section we describe a large-scale crack bridging model of microbuckle propagation. We treat the out-of-plane microbuckle as a bridged mode I crack in compression. The crack is ascribed a tip toughness G_C and a constant normal bridging stress across its flanks. The microscopic origins of the tip toughness stem from the strain energy stored in the transition

region between unbuckled and buckled fibres of the microbuckle. This is discussed in further detail by Sutcliffe *et al.* (1996). The constant crack bridging stress is associated with the phenomenon of steady state band broadening. The crack bridging model has already been presented by Sivashanker *et al.* (1996), and so only the main details are summarised here. Although the specimen used in the current study is a single edge-notch specimen, the clamping action of the wedge grips allows little rotation of the specimen ends and it is more appropriate to treat the specimen as one half of a centre-notch panel. This approximation has been verified in a previous study (Sutcliffe and Fleck, 1993).

For the single edge notch geometry of Fig. 1, the initial notch depth a_0 equals 15 mm and the specimen width b equals 50 mm. A microbuckle of length ℓ grows from the root of the notch (assumed sharp), driven by a remote applied stress σ_r. The undamaged specimen is mimicked by a rectangular panel of width $2b$ and initial notch length $2a_0$. The damaged specimen is modelled by a crack of length 2a in the centre-notched panel, where $a = a_0 + \ell$ is the sum of the initial notch length and the microbuckle length. The crack has a constant crack tip toughness G_c and a constant bridging stress of magnitude σ_b across the microbuckled region.

The stress intensity factor at the crack tip due to the applied remote compressive stress σ_r is denoted by K_r and that due to the constant bridging stress along the microbuckle length σ_b is labelled K_b. The net stress intensity factor at the microbuckle tip K_t is given by superposition of the contributions from remote loading and bridging. Thus

$$K_t = K_r + K_b \tag{1}$$

which can be re-written in the form

$$K_t = (F_r\sigma_r - F_b\sigma_b)\sqrt{\pi a} \tag{2}$$

The functions F_r and F_b are detailed in the appendix of Sivashanker *et al.* (1996).

The applied stress σ_r is predicted as a function of the microbuckle length by equating the total crack tip stress intensity factor K_t to an assumed fracture toughness K_C. In other words, the microbuckle length as a function of remote stress is assumed to be that given by the crack analogy, taking a constant crack tip fracture toughness K_C and a constant crack bridging stress σ_b. The assumed value of K_C is deduced from the measured load at microbuckle initiation.

An additional check on the crack model is made by comparing the predicted crack overlap displacement δ with the measured microbuckle width. The in-plane, mode-I crack overlap displacement δ is predicted from the remote loading and the crack bridging tractions by

$$\frac{\delta E'}{a} = U_r\sigma_r - U_b\sigma_b \tag{3}$$

where the functions U_r and U_b are calculated using weight function theory (see the Appendix of Sivashanker *et al.* (1996) for details). The constant E' is the plane stress orthotropic modulus and appears in the standard formula (Sih *et al.*, 1965),

$$G = \frac{K^2}{E'} \tag{4}$$

Here, G is the mode I strain energy release rate and K is the mode I stress intensity factor. The usual expression for E' in terms of the orthotropic elastic constants is included in Appendix A for completeness.

We define the width w of a microbuckle band at any location by the fibre length contained within the microbuckle band. The crack overlap displacement δ represents the end-shortening associated with fibre rotation in the microbuckle band. It is assumed that fibres rotate out-of plane through an angle ϕ given by $\phi = 2\beta$, where β is the orientation of the microbuckle band, as shown in Fig. 7. The condition $\phi = 2\beta$ is a statement that fibres rotate until the volumetric strain in the band vanishes (Fleck and Budiansky, 1991) and is confirmed by experimental observations of the amount of fibre rotation within a microbuckle band. The crack overlap displacement δ due to a fibre rotation $\phi = 2\beta$ within the microbuckle band of width w is given by the straightforward kinematic expression

$$\delta = w(1 - \cos\phi) \tag{4}$$

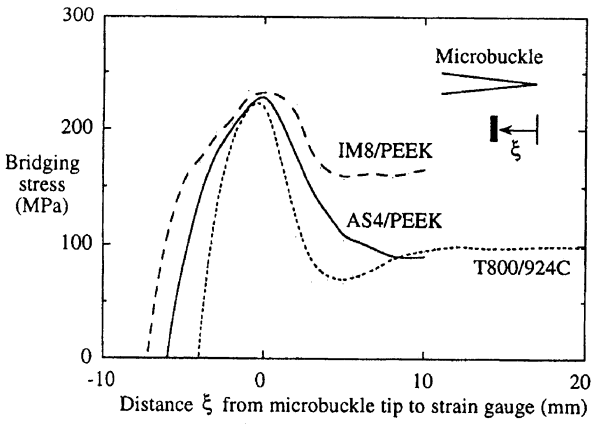

Fig. 6. - Measured bridging stress across microbuckle flanks as the microbuckle grows past the strain gauges, for the three unidirectional laminates.

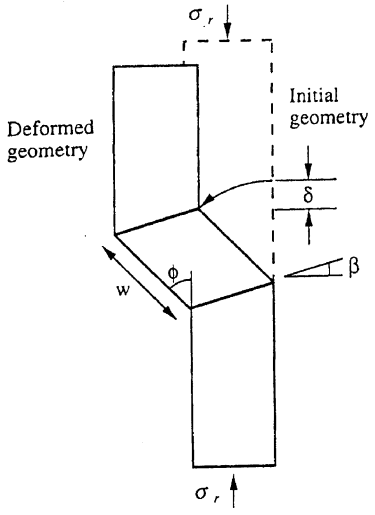

Fig. 7. - Kinematics of the microbuckle. Lock-up occurs after a fibre rotation $\phi=2\beta$.

3.5 Predictions of the crack model

The predicted collapse responses for the AS4/PEEK composite and for the IM8/PEEK composite are compared with experimental observations in Figs. 8a and 8b, respectively. A comparison of the mode for T800/924C has already been reported (Sivashanker et al., 1996). For each material, the measured remote stress for initiation of microbuckle propagation is used to infer the tip stress intensity factor K_C and the corresponding tip toughness G_C using

equation (2). These values are given in Table 1. The tip toughness G_C ranges typically from 17 - 21 kJ/m^2. We note that the G_C values of the PEEK-matrix composites are remarkably close. This is despite the fact that the AS4 fibres break during microbuckling whereas the IM8 fibres remain intact. This suggests that fibre fracture plays a relatively minor role in determining the tip toughness.

TABLE 1. - Material properties for unidirectional laminates.

Material	E′ (GPa)	K_C (MPa$\sqrt{m}$)	G_C (kJ/m^2)	β (degrees)	σ_b (MPa)
T800/924C	54.8	30.7	17.3	25	100–133
AS4/PEEK	46.0	30.3	20.0	27	100
IM8/PEEK	63.5	35.5	19.8	26	150

Predictions of the remote stress for microbuckle propagation as a function of microbuckle length are made for a range of assumed bridging stresses σ_b in Fig. 8. The shape of the crack growth resistance curve is sensitive to the level of assumed bridging stress. For example, for the limiting case of σ_b=0, predictions lead to a monotonically decreasing applied stress with increasing microbuckle length which is grossly inconsistent with experimental trends. Experimental estimates of the bridging stresses σ_b for the three different materials, taken from strain gauge measurements, are displayed in Table. 1 and the corresponding predictions match the measured collapse response quite reasonably (see Figs. 8a and 8b, and Fig. 8 of Sivashanker et al. (1996)).

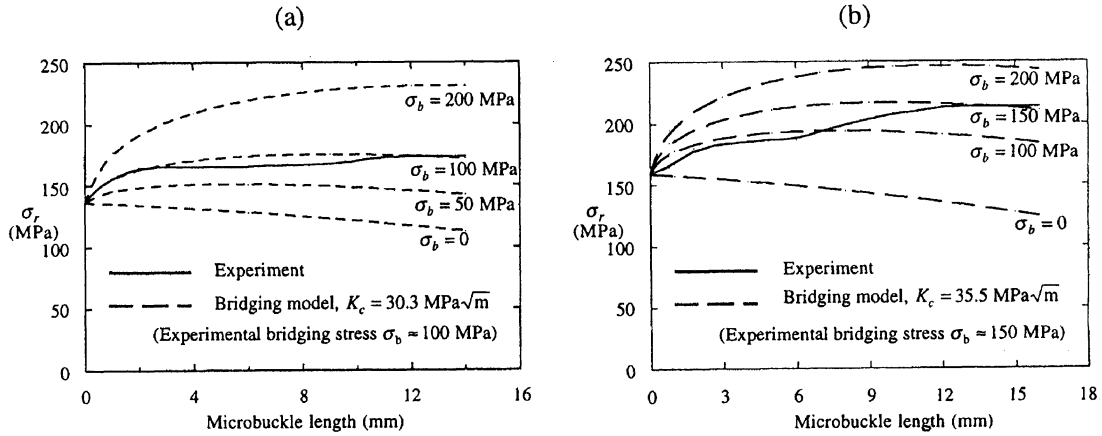

Fig. 8. - Comparison of measured collapse response with predictions of the large-scale crack bridging model for unidirectional laminates. (a) AS4/PEEK; (b) IM8/PEEK.

Further validation of the large-scale crack bridging model comes from comparing the predicted and measured shapes of the microbuckle band for all three unidirectional materials. The predictions come from equations (3), (4) and (5) using the relevant bridging stresses σ_b and measured kink band angles β (Table 1). The value of E′ is calculated from unidirectional laminate properties. Figures 6a and 6b show that the crack theory adequately predicts the observed trend of increasing kink-band widths. Similar agreement is shown for the T800/924C unidirectional material in Fig. 8 of Sivashanker et al. (1996).

4. Results for multi-directional material

4.1 Fracture mechanisms

Notched multi-directional specimens were made from the T800/924C carbon-epoxy material and were tested in the same manner as for the unidirectional specimens. The main failure mechanism was microbuckling with delamination between plies. Although the precise details depend on lay-up, the main damage mode was the same and we focus on results for the lay-up $[(\pm 45/0_2)_3]_s$. Visual examination of the side face of the laminate revealed a zig-zag fracture pattern of the outer 45° plies, see Fig. 9. This can be decomposed into splits along the 45° directions and fibre microbuckling normal to the fibre directions. A region of delamination surrounds the zig-zag microbuckle pattern, and is demarked by bright areas in Fig. 9. The progressive growth of 45° ply surface delaminations has been observed previously by Waas *et al* (1990) using holographic interferometry.

The precise nature of the microbuckling sequence was determined by terminating a test prior to catastrophic fracture and by sectioning the specimen on a succession of planes normal to the main direction of damage growth, see Fig. 9. At the tip of the damage front (section A-A, Fig. 9), microbuckling of the 0° plies is observed in the central and the two adjacent outer layers. At 6 mm behind the tip of the damage zone (section B-B, Fig. 9) microbuckling failure occurred in all unidirectional layers. The damage is more extensive with delaminations between microbuckles compared to those of Fig. 9. The microbuckles are also broader in the loading direction than nearer to the tip of the damage front. Band broadening is associated with multiple fibre fragmentation, as for the case of unidirectional T800/924C composite. For example, the central ply contains a microbuckle consisting of several kink fragments. At section C-C, 11 mm behind the microbuckle tip the individual regions of microbuckling and delamination have coalesced.

The observations above identify the most important features of the failure process to be microbuckling of the 0° plies coupled with interface delamination between dissimilarly oriented layers. The nature of the compressive damage in multi-directional composites is best idealised by a 'wing-crack analogy'. Heterogeneous brittle solids fail by local slip across a

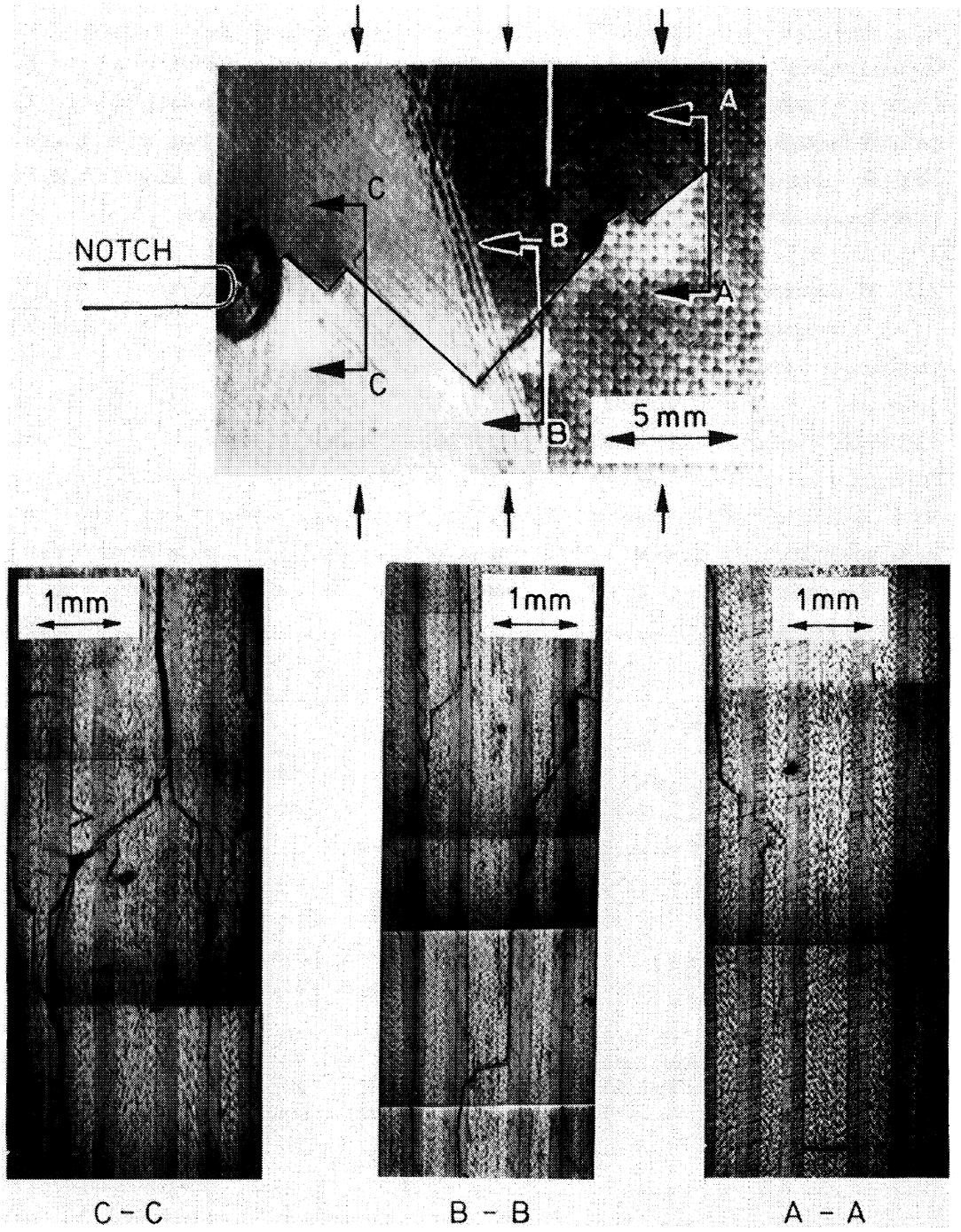

Fig. 9. - Micrographs showing damage in a T800/924C laminate of lay-up $[(\pm 45/0_2)_3]_S$ for microbuckle of length 16 mm from the notch root. The side view shows the zig-zag mode of growth of microbuckle and splits in the off-axis surface plies. Sections A-A, B-B and C-C are located at the tip of damage, 6 mm back and 11 mm back respectively. Note that the two white vertical lines are scribe lines and do not correspond to damage. Cross-section at A-A shows isolated microbuckling of the light-coloured 0° plies and limited delamination. Cross-section at B-B shows linking of microbuckled layers and some off-axis microbuckling. Cross-section at C-C shows fully connected microbuckling and delamination.

weak inclusion, with attendant mode I wing-cracks (see, for example, Sammis and Ashby (1986)). Microbuckling provides a similar sliding mode of failure, and the wing-cracks are replaced by interfacial delamination. Final failure is by the coalescence of the isolated damage zones of microbuckling in combination with delamination, as sketched in Fig. 10. The damage mode is somewhat more complicated than that described above: microbuckles develop within the off-axis 45° plies in addition to the 0° plies.

4.2 Measurements of local bridging stress and measured R-curves

Foil strain-gauges were used to measure the local bridging stresses in the wake of the propagating damage zone, in a similar manner to that described above for unidirectional specimens. A typical example is shown in Fig. 11 for lay-up $[(\pm 45/0_4)_2]_S$ of the T800/924C composite. The axial stress measured by the gauges attains a maximum value when the damage front lies adjacent to the gauge and asymptotes to an almost constant value when the damage is well past the gauges. Measurements from duplicate tests are presented for each multi-directional lay-up in Table 2. The steady state bridging stress is in the range of 2-3 times the shear yield strength of the matrix, in agreement with the measurements for unidirectional material.

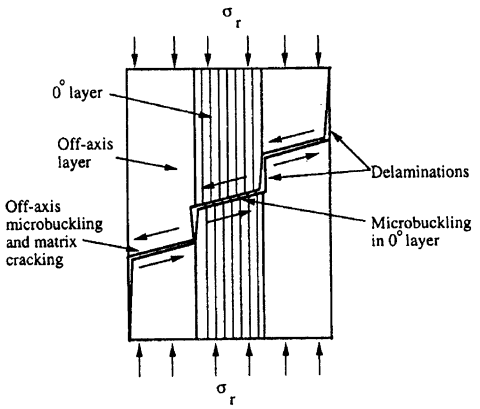

Fig. 10. - Sketch showing coalescence of microbuckles and adjacent delamination cracks

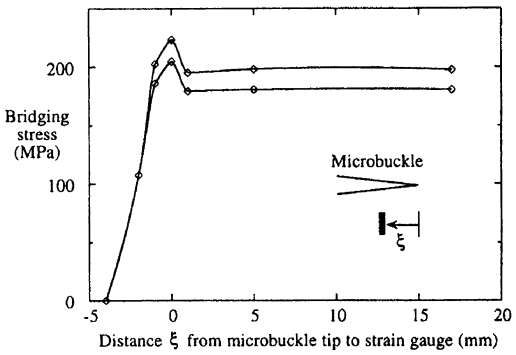

Fig. 11. - Measured bridging stress across microbuckle flanks as the microbuckle grows past the strain gauges, for the T800/924C laminate of lay-up. The two curves are for two duplicate tests.

In unidirectional material the bridging stress is associated with the band broadening phenomenon described in the preceding section. Once formed, the microbuckle continues to broaden in the fibre direction resulting in multiple kink-bands. In multi-directional material the situation is more complicated; the bridging stress appears to be associated with two mechanisms: band-broadening in the 0-degree layers and delamination crack growth from the

ends of the microbuckles. Band broadening of microbuckles was also observed in the off-axis 45° plies.

The evolution of microbuckle length with applied stress is summarised in Fig. 12 for both multi-directional and unidirectional specimens made from T800/924C material. The response is remarkably independent of lay-up. For example, the $[(\pm 45/0/90)_3]_s$ laminate contains only 25% of 0° plies yet is only 20% weaker than the other T800/924C unidirectional laminate.

TABLE 2. - Measured properties for multidirectional laminates of T800/924C.

Lay-up		Unidirectional	$[(\pm 45/0_4)_2]_s$	$[(\pm 45/0_2)_3]_s$	$[(\pm 45/0/90)_3]_s$
% of 0° plies		100	67	50	25
Measured	Expt. 1	100	180-200	170-200	120
σ_b (MPa)	Expt. 2	133	150-185	170-190	140
K_C (MPa$\sqrt{m}$)		30.7	24.5	25.8	20.7

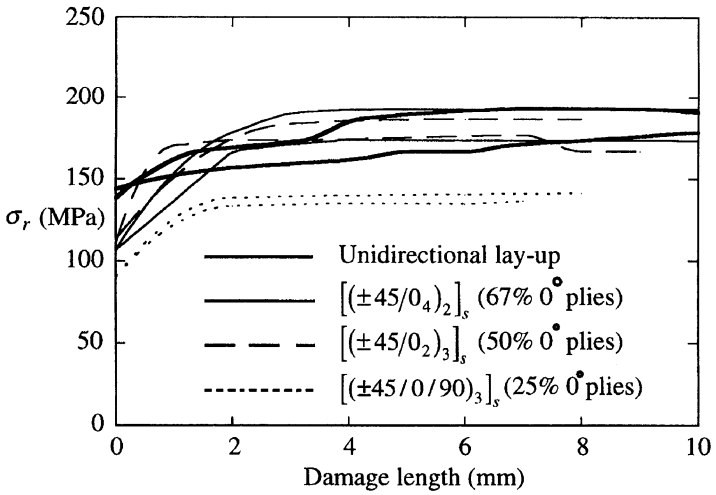

Fig. 12. - Measured microbuckle length as a function of applied stress (R-curves) for unidirectional and multi-directional T800/924C laminates.

4.3 Application of large scale bridging model to microbuckling of multi-directional specimens.

It has been demonstrated above that a large scale bridging model, based on a crack tip toughness and a constant crack bridging stress, is adequate for predicting microbuckle growth

in unidirectional carbon fibre composites. Here, the ability of this model to predict damage growth in multi-directional laminates is examined. Predictions are compared with the measured curves of microbuckle length versus applied stress in Fig. 13. The model takes as input a tip toughness to give the correct value of applied stress at microbuckle initiation. The model assumes a constant bridging stress for each laminate equal to the value measured using strain gauges. Good agreement between the model and the observed R-curve behaviour is shown for all three laminates. Values of the inferred tip stress intensity factor K_C for microbuckle propagation are summarised in Table 2.

Linear-softening bridging model

Whilst a crack bridging model with a finite tip toughness gives accurate predictions for microbuckle growth from a pre-existing sharp notch, it fails for the case of a panel containing a blunt notch such as a hole: the model erroneously predicts that an infinite remote stress is required for initiation of microbuckling in the absence of an initial flaw. Soutis *et al.* (1991) recognised this drawback and proposed an engineering model for microbuckling of multi-directional laminates in the form of a linear softening cohesive zone law. The compressive traction σ across the microbuckle is assumed to depend upon the crack overlap displacement u across the microbuckle by the linear relation:

$$\sigma/\sigma_c = (1-u/u_c) \quad \text{for} \quad 0 \le u \le u_c$$
$$\sigma = 0 \quad \text{for} \quad u > u_c \qquad (6)$$

where $2u_c$ is the critical microbuckle overlap displacement and σ_u is the unnotched strength of the laminate. Since u_c is related to the measured toughness G_c of a laminate containing a long sharp notch according to

$$G_C = \int_0^{u_c} 2\sigma du = \sigma_c u_c \qquad (7)$$

a measured value of G_C can be used to determine the appropriate value of u_c.

The general calculation method for the linear softening model has been described by Cox and Marshall (1991) and further numerical details are given by Sutcliffe and Fleck (1993). The relationship between the microbuckle length ℓ and the remote applied stress σ_r is fixed by the condition of zero tip stress intensity factor. The linear softening model is used to predict the observed collapse responses for multi-directional material: predictions are included in Fig. 13. The cohesive zone model predicts that the applied stress attains a maximum at a microbuckle length of about 2 mm, and a softening behaviour thereafter. In contrast, the measured collapse response (and the crack bridging model invoking a tip toughness and constant crack bridging stress) give a monotonically hardening behaviour with microbuckle extension. In broad terms, however, the cohesive zone model gives an acceptable prediction of the maximum stress carried by the specimen, and is adequate for the early stages of microbuckle growth (e.g. the first few millimetres from the notch root). It has already been shown (Soutis, Curtis and Fleck, 1993; Fleck, Jelf and Curtis, 1995b) that the cohesive

zone model gives useful predictions of compressive strength for multi-directional laminates containing a central hole.

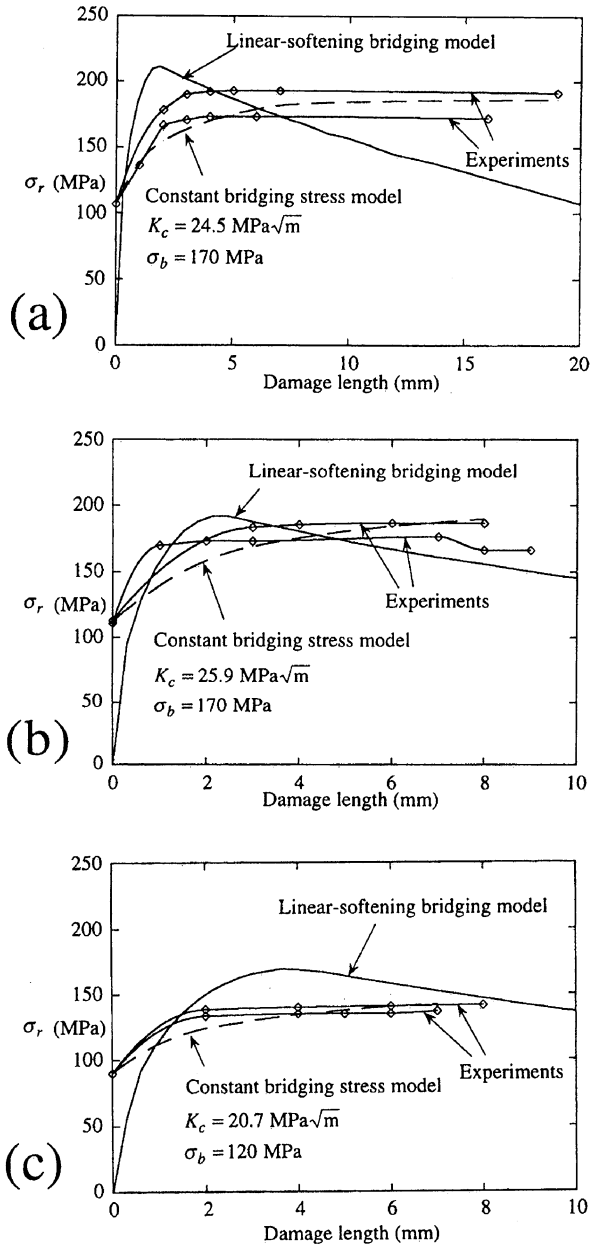

Fig. 13. - Comparison of measured and predicted R-curves for (i) constant bridging stress model with a constant tip toughness and (ii) cohesive zone model with a linear softening law. (a) lay-up $[(\pm 45/0_4)_2]_s$, (b) lay-up $[(\pm 45/0_2)_3]_s$, (c) lay-up $[(\pm 45/0/90)_3]_s$.

5. Concluding discussion

An experimental technique has been developed to allow for the detailed observation of microbuckle growth in unidirectional and multi-directional carbon fibre composites. Unidirectional laminates fail by out-of-plane microbuckling; the shape and propagation behaviour of the microbuckle is similar to that of a crack with a constant crack tip toughness and a constant bridging stress. The magnitude of the compressive bridging stress across the microbuckle is 2-3 times the shear yield strength of the composite in agreement with the predictions of Budiansky *et al.* (1997). It is found experimentally that fibre strength has a very minor effect on the propagation behaviour of a microbuckle.

Multi-directional laminates of T800/924C carbon-epoxy fail in compression by microbuckle growth in the 0° and 45° plies with attendant delamination of ply interfaces. The damage mode is reminiscent of wing-crack formation in brittle heterogeneous solids. As for the unidirectional material, a crack model with a constant crack tip toughness and a constant bridging stress gives accurate predictions of damage growth as a function of applied stress. The measured values of tip toughness and bridging stress are remarkably insensitive to the volume fraction of 0° plies.

The linear softening cohesive zone model of Soutis *et al.* (1991) gives adequate predictions of compressive strength for multi-directional laminates containing a sharp notch. Although it is less accurate than the crack bridging model invoking a crack tip toughness the Soutis *et al.* (1991) approach has the virtue that it gives reasonable predictions for both unnotched laminates and for laminates containing a hole.

Acknowledgements

The authors are grateful to Dr. Y.D.S. Rajapakse (US Office of Naval Research, grant 0014-91-J-1916) for financial support. The Ph.D. support of S.S. from the Nanyang Technological University of Singapore (NTU), School of Mechanical and Production Engineering is gratefully acknowledged.

APPENDIX A

The plane stress orthotropic modulus E' in equation (4) can be computed from laminate properties such that

$$E' = \lambda^{1/4}\left\{\frac{(2E_1E_2)}{1+\rho}\right\}^{1/2} \tag{A1}$$

where

$$\lambda = \frac{E_2}{E_1}, \qquad \rho = \frac{\sqrt{E_1 E_2}}{2G_{12}} - (\nu_{21}\nu_{12})^{\frac{1}{2}} \quad \text{and} \quad \nu_{12} = \frac{E_1}{E_2}\nu_{21} \tag{A2}$$

Subscripts 1 and 2 refer to directions perpendicular and parallel to the fibre direction respectively. E is Young's modulus, G_{12} is the shear modulus and ν is the Poisson's ratio. The elastic constants λ and ρ are non-dimensional material parameters to characterise the degree of orthotropy (Suo *et al.*, 1991). For an isotropic material of Young's modulus E, $\rho = 1$, $\lambda = 1$ and $E' = E$.

Suo *et al* (1991) have developed an orthotropy rescaling technique whereby isotropic solutions may be used as an approximation for orthotropic materials provided certain conditions are met. The technique rescales the geometry and boundary conditions of the original orthotropic problem with a function of λ; this transforms the problem to an equivalent isotropic one, for which established solutions exist. Using this technique Bao *et al* (1992) have catalogued the stress intensity factors of various notched unidirectional specimens. With materials for which ρ=1, the functions F_r, F_b, U_r and U_b (using weight function analysis) can be used immediately. But for the current polymer matrix unidirectional composites $\rho \neq 1$ as listed below. Therefore a correction for orthotropy is required.

Table A1. Orthotropy values (ρ, λ) for unidirectional laminates of current study

Material	T800/924C	IM8/PEEK	AS4/PEEK
λ	17.4	23.2	13.0
ρ	3.1	4.2	3.1

Bao *et al* (1992) have demonstrated through finite element analysis that the effect of λ is negligible for a sufficiently long and narrow specimen. They found that the stress intensity factors of notched specimens approach their isotropic value when $\lambda^{1/4} h/2b \geq 2.0$. With h = 245 mm and b = 50 mm for the current specimen geometry, this requirement is more than satisfied . The ρ dependence is taken into account by applying a multiplicative correction factor[1] $Y(\rho)$ to the K calibration following Bao *et al* (1992):

$$Y(\rho) = \left(1 + 0.1(\rho - 1) - 0.016(\rho - 1)^2 + 0.002(\rho - 1)^3\right)\left(\frac{2}{1+\rho}\right)^{\frac{1}{4}} \tag{A3}$$

[1] An error in the correction factor has been corrected via private communication with Bao (1992)

REFERENCES

BAO, G., HO, S., FAN, B. and WANG, T. C, 1992, The role of material orthotropy in fracture specimens for composites, *Int. J. Solids Struct.*, **29**(9), 1105-1116.

BUDIANSKY, B., FLECK, N. A. AND AMAZIGO, J. C., 1997, On compressive kink-band propagation, *manuscript in preparation.*

COX, B. N. and MARSHALL, D. B., 1991, Stable and unstable solutions for bridged cracks in various specimens, *Acta Metallurgica et Materialia*, **39**(4), 579-589.

FLECK N. A. and BUDIANSKY B., 1991, Compressive failure of fibre composites due to microbuckling , in *Inelastic Deformation of Composite Materials*, ed. G. J. Dvorak, Springer-Verlag, 235-274.

FLECK N. A., DENG L. and BUDIANSKY B., 1995a, Prediction of kink width in compressed fiber composites. *ASME J. Applied Mechanics*, **62**(2), 329-337.

FLECK N. A., JELF P. M. and CURTIS P. T., 1995b, Compressive failure of laminated and woven composites, *ASME J. Composites: Technology and Research*, **17**(3), 212-220.

FLECK N. A., 1997, Compressive failure of fibre composites, *Advances in Applied Mechanics*, **34**, Academic Press, ed. J.W. Hutchinson and T.Y. Wu, 43-118.

MORAN, P.M., LIU X. H. and SHIH, C.F., 1995, Kink band formation and band broadening in fiber composites under compressive loading. *Acta metall. mater.*, **43**(8), 2943-2958.

SAMMIS, C.G. and ASHBY, M. F., 1986, The failure of brittle porous solids under compressive stress states, *Acta Metallutgica*, **34**(3), 511-526.

SIH, G. C., PARIS, P. C. and IRWIN, G. R., 1965, On cracks in rectilinearly anisotropic bodies *Int. J. Fract. Mech.*, **1**(3), 189-203.

SIVASHANKER S., FLECK N. A. and SUTCLIFFE M. P. F., 1996, Microbuckle propagation in a unidirectional carbon fibre - epoxy matrix composite. *Acta Materiala*, **44**(7), 2581-2590.

SOUTIS C., FLECK N. A. and SMITH P. A., 1991, Failure prediction technique for compression loaded carbon fibre-epoxy laminate with open holes, *J. Composite Materials*, **25**(11), 1476-1498.

SOUTIS C., CURTIS P. T. and FLECK N. A., 1993, Compressive failure of notched carbon fibre composites. Proc. Roy. Soc., **440**, 241-256.

SUO, Z., BAO, G., FAN, B. AND WANG, T.C. 1991, Orthotropy rescaling and implications for fracture in composites, *Int. J. Solids Struct.*, **28**(2), 235-248

SUTCLIFFE M. P. F. and FLECK N. A., 1993, Effect of geometry upon compressive failure of notched composites. *Int. J. Fracture*, **59**, 115-132.

SUTCLIFFE M. P. F. and FLECK N. A., 1994, Microbuckle propagation in carbon fibre - epoxy composites. *Acta Metallurgica and Materialia*, 42(7), 2219-2231..

SUTCLIFFE, M. P. F., FLECK, N. A. and XIN, X. J., 1996, Prediction of compressive toughness for fibre composites. *Proc. Roy. Soc. Lond.* , **A452**, 2443-2465.

WAAS A. M., BABCOCK C. D., JR., and KNAUSS W. G., 1990, An experimental study of compression failure of fibrous laminated composites in the presence of stress gradients", *Int. J. Solids Struct.*, **26**(9/10), 1071-1098.